



OPEN

Injectable 3-D Fabrication of Medical Electronics at the Target Biological Tissues

Chao Jin¹, Jie Zhang¹, Xiaokang Li¹, Xueyao Yang¹, Jingjing Li¹ & Jing Liu^{1,2}

¹Department of Biomedical Engineering, School of Medicine, Tsinghua University, Beijing 100084, China, ²Beijing Key Lab of Cryo-Biomedical Engineering and Key Lab of Cryogenics, Technical Institute of Physics and Chemistry, Chinese Academy of Sciences, Beijing 100190, China.

Received
10 July 2013

Accepted
20 November 2013

Published
6 December 2013

Correspondence and
requests for materials
should be addressed to
J.L. (jliubme@tsinghua.
edu.cn)

Conventional transplantable biomedical devices generally request sophisticated surgery which however often causes big trauma and serious pain to the patients. Here, we show an alternative way of directly making three-dimensional (3-D) medical electronics inside the biological body through sequential injections of biocompatible packaging material and liquid metal ink. As the most typical electronics, a variety of medical electrodes with different embedded structures were demonstrated to be easily formed at the target tissues. Conceptual *in vitro* experiments provide strong evidences for the excellent performances of the injectable electrodes. Further *in vivo* animal experiments disclosed that the formed electrode could serve as both highly efficient ECG (Electrocardiograph) electrode and stimulator electrode. These findings clarified the unique features and practicability of the liquid metal based injectable 3-D fabrication of medical electronics. The present strategy opens the way for directly manufacturing electrophysiological sensors or therapeutic devices *in situ* via a truly minimally invasive approach.

For decades, implantable medical devices (IMDs) have been serving as a highly efficient way to monitor and treat seriously diseased physiological conditions inside the biological body. Among the many developed typical devices, the pacemakers, defibrillators, cochlear implants, drug monitoring and delivery systems are especially contributing significantly to the management of a wide spectrum of diseases, such as Parkinson's disease, hearing disorders, diabetes, cardiac arrhythmia and so on¹⁻⁶. Over the past few decades, millions of people have benefited from such inventions to maintain their life-critical functions²⁻⁴. Meanwhile, it also raised serious concerns over the tremendous practices. For example, the high cost of the rigid IMD and the discomfort it caused, the complicated implantation surgery and follow-up maintenance etc. often lead to a heavy burden to the patients^{7,8}. Generally, a typical implantation surgery would include such processes like incision, device implantation and suture which however will inevitably bring about big physical pain and emotional stress to the patients, as partially reflected by Fig. 1a. In addition, the related complication (e.g. infection) induced by the IMDs further adds potential risks to the patients, although many attempts have been made to improve the biocompatibility of the devices⁹⁻¹⁴. Taken together, these factors kept challenging the widespread application of IMDs. Therefore, for many years, there has always been an urgent need to develop as friendly as possible IMDs with higher performances, e.g. cost-effective, easy-operation, minimally invasive feature and miniaturization etc.^{15,16}.

Here, we report a fundamentally innovative way for directly making 3-D compliant medical electronics inside the biological tissues through injecting the conductive liquid metal (see Fig. 1b) and the allied packaging material to the target. Different from the conventional surgical principles, the present method is based on a minimally invasive injection process which therefore will significantly relieve serious sufferings of the patients. The recent emergence of the liquid metal based printed electronics and fabrication is drawing increasing attentions among academia and industry¹⁷⁻²³. Owing to the unique merits of the liquid metal such as low melting temperature, well controlled wettability, and high electrical conductivity, such material offers a cost-effective and convenient way for the present purpose. In this study, focusing on the electrode, a most typical medical electronics in biomedical engineering area, we illustrate the 3-D molding and working of a series of injectable electrodes with embedded complex structures. Both *in vitro* and *in vivo* experiments regarding the electronic components with different shapes were performed. The feasibility of the 3-D electronic fabrication through directly injecting the liquid metal and the packaging gel to the target tissues was demonstrated. This study opens a highly desirable minimally invasive way for future practices of transplantation medicine.

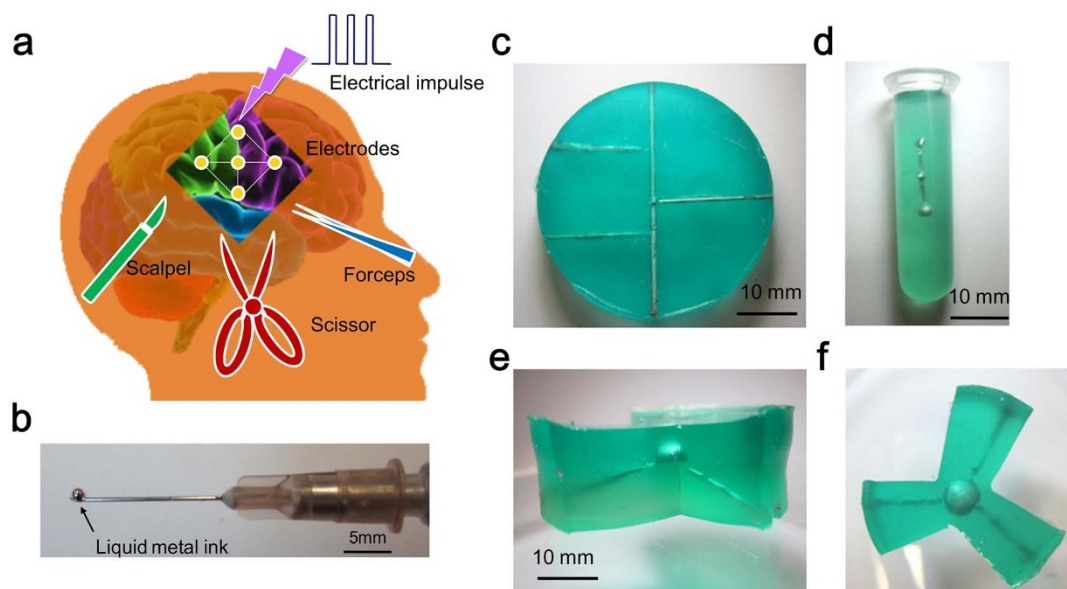


Figure 1 | Profiles for injectable 3-D fabrication of medical device. (a) Schematics for conventional surgery in implanting electrode for brain stimulator. (b) A liquid metal droplet on the tip of entry needle. An electric wire network (c), a node-shaped electronic component (d), and a 3-D triangle frame electronic component (e) and (f) fabricated by injecting the liquid metal into the packaging domains.

Results

Injectable fabrication of 3-D electronics. Starting from making a variety of matching electronics inks especially liquid metal (further details regarding the used materials were described in Methods section) and injecting them into the packaging domains, we could finally fabricate various kinds of functional electronic devices or components, such as electric wire network (Fig. 1c), node-shaped electronic component (Fig. 1d) and 3D triangle frame electronic component (Fig. 1e, f). Fig. 2 and Methods section gave more details about the fabrication procedure. Clearly, with the identified excellent flexible materials, i.e. liquid metal and gelatin, it would allow the compliant working of a soft and comfortable medical device inside the biological body which meanwhile will cause no injury even discomfort to the directly-contacting organs. Further, in contrast to the conventional implanted devices, the patients injected with electronic elements can be allowed to freely take the MRI (Magnetic Resonance Imaging) examination owing to the adopted liquid metal's non-magnetic property. This is rather beneficial for the practices of medical examination.

To evaluate the electronic properties, we firstly fabricated an electrode through the injection way in a 1 ml pipette tip, as depicted in

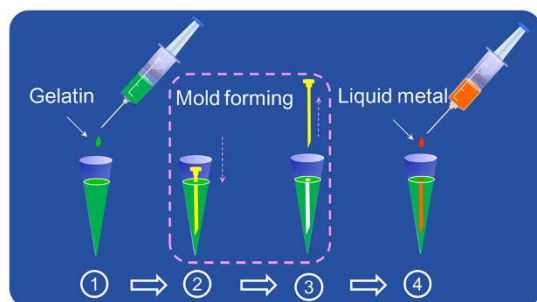


Figure 2 | Alternative strategies for making implantable bio-electrode through directly injecting liquid metal and allied packaging material inside a pipette tip. Here, (1) denotes the formed packaging domain; (2) and (3) represent the fabrication process of electrode mode; (4) denotes the formed electrode within the packaging domain by injecting with the GaInSn-based liquid metal ink.

Fig. 3a. The impedance measurements indicate that the formed electrode has an overall electrical resistance of 16×10^3 ohm; meanwhile, the resistivity of the liquid metal is only about 200 ohm. It is such a large resistivity of the packaging material that significantly reduced the injected composite's conductivity which is beneficial for isolating the electronics from the outside. The special function and application determines the electrical properties of conventional medical electrodes. It has been reported that clinical impedance measurements for deep brain stimulation (DBS) electrodes in patients ranges from 500 ohm to 1500 ohm²⁴. In this respect, the current injected liquid metal-based electrode well meets the requirements of DBS in conducting the electrical signals.

Further tests in demonstrating the electronic performance of the formed electrode have been implemented (see Fig. 3b, c and Methods section for the test setup). The input signal is a typical wave square signal with an amplitude of 1 V, frequency of 100 Hz and duty ratio of 20% respectively, as shown in Fig. 3d. As seen from the output signal's basic features (Fig. 3e), a good performance of electrical conduction has been realized. Meanwhile, the output signal also appears to have certain faint noises and a slight baseline drift. The electrode structure and the used packaging material may partially contribute to the distortion of original signal. Nevertheless, all the attempts demonstrated the feasibility of fabricating an electrode by means of liquid metal injection and in-situ packaging. The results also revealed the excellent electronic property of the injected electrode.

In vitro demonstration experiments. Further in vitro experiments for fabricating the injected electrode within the porcine tissues have also been conducted. Figure 4 illustrates the fabrication procedure as described in the above section. During the procedure of (2) and (3), a syringe needle with a diameter of 1 mm was employed to shape the electrode mold. And through injecting the GaInSn-based liquid metal ink, an electrode with diameter of 1 mm was fabricated in the final step of (4).

Figure 5a presents the cross-sectional photograph of the injected electrode within the porcine tissue. As observed, a packaged electrode with volume of 353.25 mm³ has been fabricated, in which the main part composed of liquid metal ink is a proximate cylinder with length of 12 mm and radius of 0.5 mm, respectively. The formed

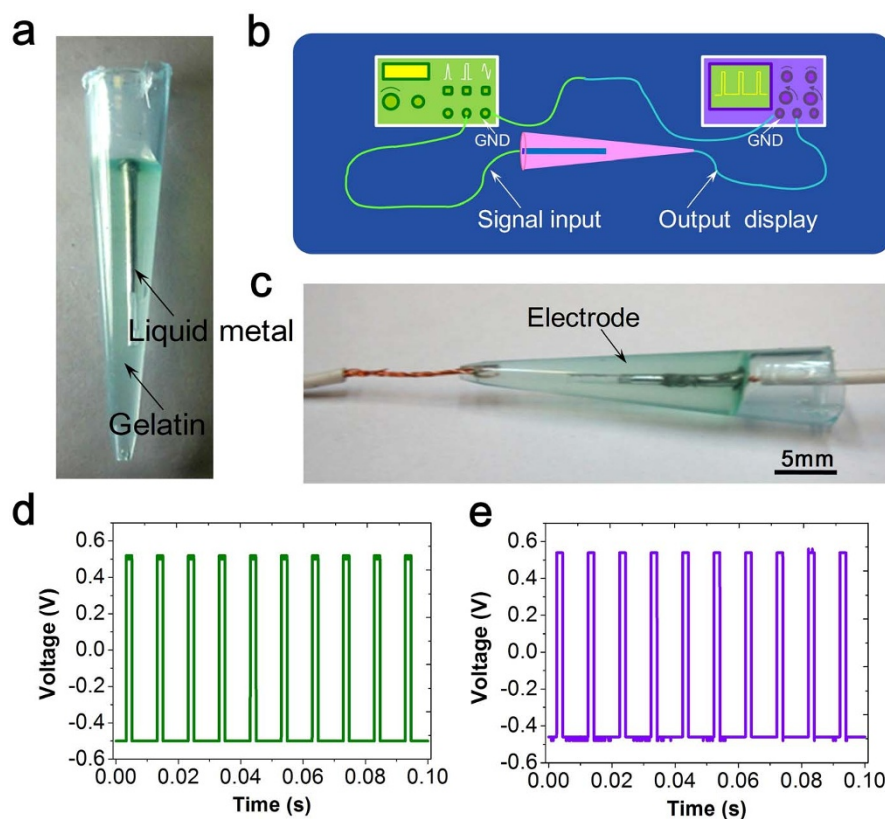


Figure 3 | Visualization experiments to characterize injectable packaged electrode in a transparent pipette tip. (a) The formed electrode in a 1 ml pipette tip. Schematics (b) and (c) are for electronic tests of the electrode. The input signal (e) and the measuring result (d).

electrode meets well the standards of DBS electrode, e.g. cylindrical Medtronic 3387/3389 DBS electrode with a radius of 0.64 mm^2 . Figure 5b, c indicate the surface topography of the formed electrode, provided by the SEM images. The underlying interaction may lead to the irregular boundary between the packaging material and the pock tissues. By contrast, the packaged liquid metal shows uniform distribution within the packaging domain. It also supports that the injectable molding method could efficiently fabricate a well-shaped electrode. The electrical tests indicate that, in comparison with the input signal (Fig. 3d), the output signal again exhibits the alike features, including the amplitude, frequency and duty ratio (Fig. 5d). Overall, these results demonstrated the feasibility of using the injected electrode as a good media to administrate the desirable stimulation into the biological tissue.

In vivo working of injected medical electronics. To test the working behaviors of the injected electronics, in vivo experiments were also

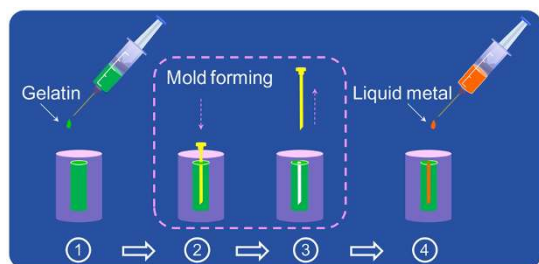


Figure 4 | Alternative strategies for making implantable bio-electrode through directly injecting liquid metal and allied packaging material inside the porcine tissue. Here, (1) denotes the formed packaging domain; (2) and (3) represent the fabrication process of electrode mode; (4) denotes the formed electrode within the packaging domain by injecting the GaInSn-based liquid metal ink.

implemented as indicated by Fig. 6 (further experimental methods and implementation are described in Methods section). Here, we selected a mouse weighting 20.0 g as the subject. The animal study has been approved by the Ethics Committee of Tsinghua University, Beijing, China under contract [SYXK (Jing) 2009–0022]. Figure 6a presents the schematic illustration of the experimental setup for measuring the mouse ECG signal. The injected electrode with length of 5 mm is fabricated in the left side of the thorax near the left upper limb, as depicted in the dissection photograph (Fig. 6b, c). It can also be found that the resulting wound to the mouse as well as that of drug injection, is extremely small that can be ignored. Figure 6d provides the recorded ECG signals of the experimental mouse at 5 min and 10 min after injecting the anesthesia. As observed, the recorded signals also show very similar features with a typical mouse ECG, including a P wave, a QRS complex and a ST segment^{25,26}. The magnitude of 0.3 mV appears somewhat slightly weak which may be caused by two primary factors, i.e. the electronic properties and lead mode of the injected electrode. In addition, some quantitative indexes have also been estimated, including the heart rate of 630 bpm and QT interval of 66.0 ms. All these results indicate relatively good accordance with the previously reported results of mouse ECG^{25,26}.

The formed electrode has also been applied to introduce an electrical stimulation to the test mouse (see Methods section for more experimental details). The evident changes of the mouse ECG can be observed when the magnitude of the stimulation signal is set as 0.6 mV, as plotted in Fig. 6e. And the electrical stimulation mainly appears at the PQ interval of the mouse ECG. It also results in a phenomenal increase of heart rate. When the magnitude increases to 1.2 mV, despite of the magnitude, the similar phenomenon of physiologic response has been observed. However, when the magnitude increases to 1.3 mV, the physiologic response induced by the electrical stimulation seems disappeared in the recorded ECG. This can

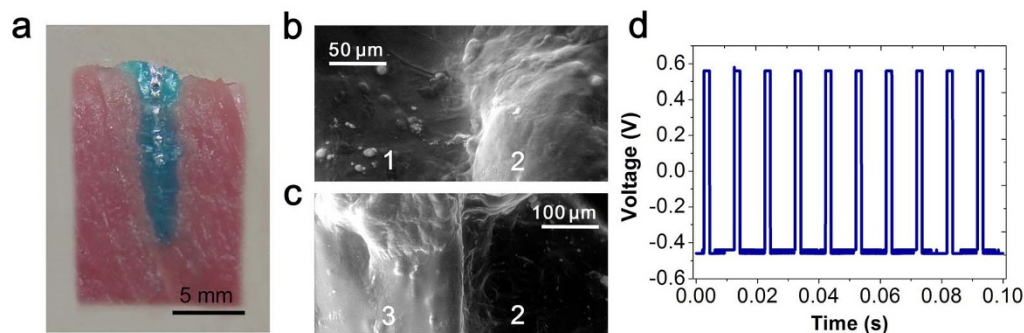


Figure 5 | Injectible electrode within the in vitro porcine tissues. The cross-sectional photograph (a) of the shaped injected electrode. The micro-boundary SEM images (b) and (c); here, symbols 1, 2, 3 denote the pock tissues, packaging material and liquid metal ink, respectively. The electronic test results (d) for the formed electrode.

be interpreted as that the increase of electrical stimulation induced the spasm of the mouse muscle which thereby cannot conduct the stimulation signal to the body.

In addition to the above demonstrations on the electrical stimulation on the targeted tissues, the typical frog's sciatic nerve model has also been adopted to test such injectable electrode's diverse performances in conducting the electrical-stimuli signals to the nerves (see Fig. 7a and methods section for more experimental details). In the experiments, an interceptive lower part of a bullfrog body was firstly prepared. And we then carry on the fabrication procedure of the injected medical electrode within the frog's tissues, as described in the above paragraph. The two injected electrodes are respectively fabricated in the left and right side of the sciatic nerve near the femur (Fig. 7b). Furthermore, the X-ray image was introduced to monitor the molding and contrast effects of such injectable electrode (Fig. 7c). During the fabrication of injectable electrode, three experiments have been sequentially implemented, including (1) The control experiment that directly loads the electrical stimulations to the frog's tissue; (2) The experiment I that loads the electrical stimulations to the nerves by the injected packaging material, i.e. gelatin; (3) The experiment II that loads the electrical stimulations by the injectable

electrode (see supplementary materials for more details). In the control experiment, one can observe that the loaded input signal with voltage amplitude of 2 V induces a contraction of local muscles at a certain frequency (see Supplementary Movie 1,2); while a stronger contraction would occur when the amplitude increases to 4 V (see Supplementary Movie 3,4). In the experiment I, the positive and negative leads of the electric-stimuli signal are connected to the injected gelatin, respectively. Same as the control experiment, varying degrees of local muscles' contractions were just observed (see Supplementary Movie 5 ~ 8); and such results suggest the good insulativity of the used gelatin. As for the experiment II, the positive and negative leads of the electric-stimuli signal are connected to the injectable electrodes, respectively. The results indicate that the injectable electrode could serve as a good medium to conduct electrical stimulations to the sciatic nerve, and hence induce the contraction of the gastrocnemius muscle (see Supplementary Movie 9 ~ 12).

Discussion

Both the above in vitro and in vivo experimental results have demonstrated the practicability of the new tool for flexible electrophysiology research. In the coming time, a high precision control on the sizes of

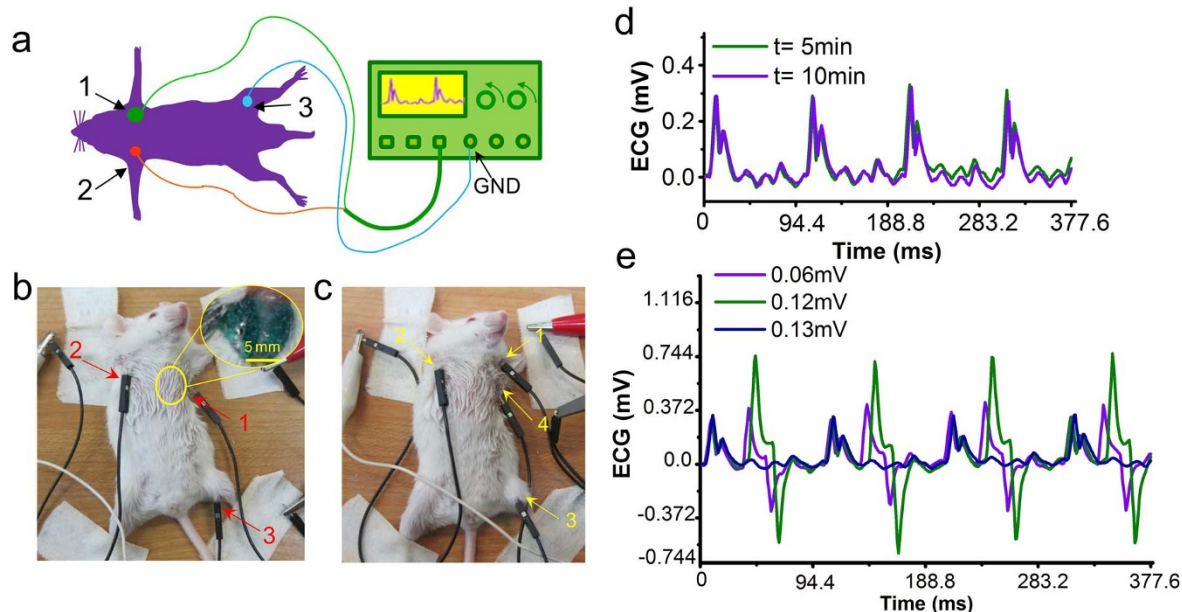


Figure 6 | Animal tests on electrode injected inside the mouse body. (a),(b) Schematics of in vivo experiment for measuring the mouse ECG signal using the injected electrode. Illustration (c) for conducting an electrical stimulation to the experimental mouse. (d) The recorded ECG signal of experimental mouse at 5 min and 10 min after anesthesia. (e) The recorded ECG signals of experimental mouse undergoing a 10 Hz electrical stimulation with magnitude of 0.6 mV, 1.2 mV and 1.3 mV, respectively.

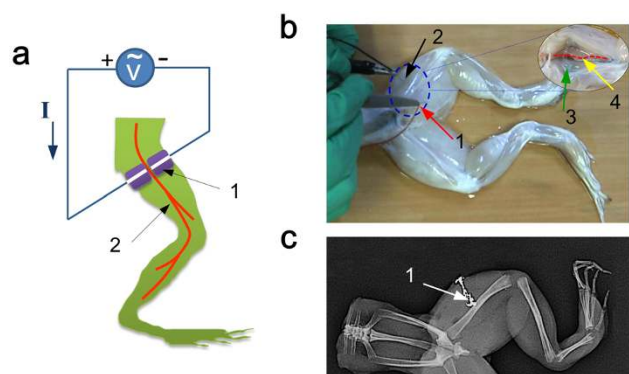


Figure 7 | Nerve electrical stimulations based on the injectable electrode. (a) Schematic of in vivo experimental setup for loading the electrical stimulations to the sciatic nerve of a frog; here symbols 1, 2 denote the fabricated electrode and sciatic nerve, respectively; (b) Illustration for the electrical stimulation to the frog's sciatic nerve; the inset is the topography of the frog's tissue with sciatic nerve and injectable electrode; here symbols 1 and 2 are respectively the positive and negative leads of the electrical input signal, symbols 3 and 4 respectively denote the injectable electrode and sciatic nerve. (c) X-ray image of the injectable electrode inside the targeted tissue of the frog's leg; symbol 1 represents the injectable electrode.

the injected electrode can be very possible through robot controlled injection and fabrication. This may add further values on the electrode's working performance in conducting electrical signal. Actually, the employed packaging material's solidification offers essential conditions for molding the injected electrode. Thus, an excellent packaging material may be the key for such purpose. The currently adopted gelatin is still not efficient enough in quickly shaping a prescribed packaging domain because of the existing solution flow within the biological tissue. Potential attempts may include adding a curing agent (e.g. mTG enzyme) and trying more materials, such as compositions of Alginate, GaCO_3 and GDL (Glucono Delta Lactone). Further, the anti-degradability of packaging material plays a partial role in determining practices of the injectable electronics. The gelatin used here can be selected as a packaging material for short term use purpose (e.g. DBS) due to its degradability within the biological body²⁷. Other than gelatin, some other packaging materials can also be employed. For example, the chemically cross-linking gelatin (e.g. mixed with genipin) would have a longer degradable interval; thus can be considered as a packaging material for a longer term running^{28–30}. Besides the material optimization, technological innovation is another way to improve the current fabrication performance. For example, a special injector with two-layer concentric circles structure can be designed, where, the inner layer is filled with the liquid metal ink and the other is the zone for packaging material which can thus well control the electrode property without the molding procedure. In addition, the league with automation control technique, e.g. surgical robot, is a promising route to replace manual injection. Finally, calibration on the electrode is always useful for guaranteeing an accurate electronics therein. Overall, a predefined electronic component or device can be flexibly available in the coming time.

Notably, safety is an important concern since a foreign substance may induce a series of underlying biological effects (e.g. potential toxicity) to the biological body. In this study, the formed electrode serves as an embedded structure of which the electronic element is wrapped in the packaging domain. As is well known, the gelatin possesses good biocompatibility and biodegradability. And the liquid metal electrodes made by gallium (Ga) and gallium-indium (GaIn) alloys have been demonstrated to own good biocompatibility to the hippocampal neurons³¹. In addition, the gallium or its alloys have

been widely used in medical practices with safety well verified. For example, gallium alloys has been employed as a restorative material in dentistry³²; and Ga-67 scintigraphy is a classical medical imaging modality^{33,34}. Besides, the stannum (Sn) has also been demonstrated to possess good biocompatibility to the biological body and widely utilized as the dental materials³⁵. Moreover, the embedded structure isolates the liquid metal from directly contacting with the tissues. Therefore, such double insurances guarantee the safety of the biological body with injected electrode. As is well known, the inflammation is a key issue in the implanted systems. With highly compliant feature enabled by the present conformable electronics, the liquid metal based transplantable medical electrodes would better tackle the inflammation issue than that in a conventional rigid transplanted device. Besides, when the injected electronics reached the end of its service life, the injected material can be possibly drained away from the body via a medical syringe or self-priming pump under the guidance of medical image system. Overall, the present method implies huge potential in biomedical field especially given its future improvement.

In summary, the liquid metal based 3-D injected fabrication technique opens the way for minimally invasive medical implantation. It offers a much superior tool in a variety of biological and medical applications, for instance fabricating a RFID (Radiofrequency Identification) (Fig. 8). Through a precise control of the injector's shifting and injection speed, a much complex RFID antenna can be easily fabricated inside the biological body. Therefore, taking more time and using additional injectable electronic inks with controllable melting, desired conductive, semi-conductive, or just isolating properties, the basic approach as initiated by the current 3-D fabrication method allows in principle making various electronic devices within the target tissues, which is an evident progress over conventional destructive implantation surgery. As a truly minimally invasive approach, this method would help refresh people's basic understandings on biomedical transplantation science and is expected to be well adopted for future researches and practices.

Methods

Materials for injectable fabrication of 3-D electronics. We used the liquid metal, i.e. GaInSn alloy (weight percent, Ga 67.0%, In 20.5%, Sn 12.5%) with the melting temperature of 283.0 K as the injectable electronic ink. The biocompatible gelatin was selected as the packaging material, owing to its excellent bio-degradable and injectable properties. A green dye (Amresco, Beijing Blodes Biotechnology Co., Ltd, Beijing, China) has also been employed to enhance the identification of the used packaging material.

Fabrication methods of 3-D injectable electronics. Figure 2 and Figure 4 present the schematic illustrations for the fabrication procedure of the injected electrode within the body. Detailed descriptions are as follows. All the complex 3-D electronics is

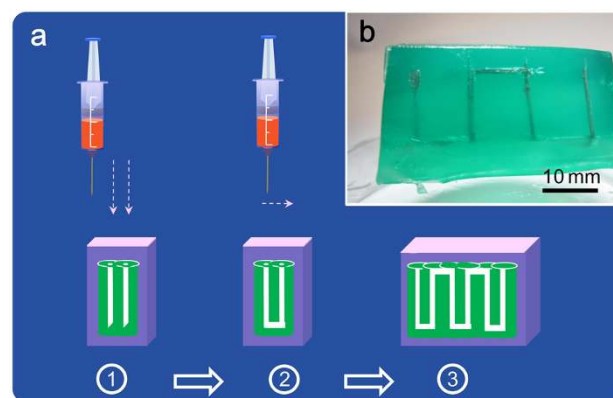


Figure 8 | Profiles for injectable 3-D RFID antenna. (a) Schematic illustration for the fabrication procedure of injected RFID antenna within the biological tissue. (b) A 3D RFID antenna fabricated by injecting the liquid metal into the packaging domains (i.e. in green color).



fabricated by using the clinical syringe as the injection tool. Firstly, fill a 10 ml syringe with 5 ml packaging material solution (mass fraction of 25.0%). And then vertically inject the solution into the target region at a rate of 1 ml/s. After removing the syringe, insert the syringe needle along the injection direction to shape a mold of electrode. About 3 ~ 5 min later, slowly remove the syringe needle and a three-dimensional packaging domain would be formed. Next, fill a 5 ml syringe with 2 ml GaInSn-based liquid metal ink and inject the ink into the electrode mold at a rate of 0.5 ml/s. Ultimately, an injected electrode can be fabricated. Using clinical syringe as the injection tool for fabricating complex 3-D object is the basic step of the present method. In fact, the size of the final object in the body can be either large or small, depending on the operation of the syringe needle and the injected amount/configuration of the liquid metal. All these difficult tasks request only a single or multiple injections.

Electronic tests for the injectable electrode. To test the electronic performance of the formed electrode, the digital signal generator (YB1610, Jiangsu Lvyang Electronic Instrument Group Co., Ltd, China) was employed to supply the stimulation signal; and the display of output signal can be performed by the digital oscilloscope (MSO2014, Tektronix, USA). The surface morphology of the formed electrode within the pock tissue was observed using environment scanning electron microscope (FEI Quanta 200, FEI, Czech). Figure 3b, c present the schematics for the electronic measurements of the injectable electrode, including the equipment setup and testing methods. Here, the digital generator and the digital oscilloscope are respectively utilized to generate the input stimulation signal and display the output signal. Two copper wires with a diameter of 0.5 mm have been connected with the two ports of the formed electrode. Meanwhile, the positive lead of digital signal generator is connected to the formed electrode and the negative lead was directly connected to the GND. The GND here is utilized as the counter electrode.

In vivo experiments for testing the working performance of the injectable medical electronics as ECG electrode. During the in vivo mouse experiments, electrophysiological applications where the injectable electronics serves as an ECG (Electrocardiograph) electrode and a stimulator electrode, respectively were administrated. A MPA acquisition and analysis system (MPA2000, Shanghai Alcott Biotech Co. Ltd., China) was utilized to measure and record the ECG signal of the experimental mouse.

During the in vivo experiment, the test mouse was anesthetized via intraperitoneal injection of pentobarbital sodium with a mass fraction of 1%. When vital signals became stable, the mouse was comfortably put on the operating table. And we then carry on the fabrication procedure of the injected medical electrode within the mouse, as described in the above paragraph. The injected electrode is fabricated in the left side of the thorax near the left upper limb (Fig. 6b). A lead-II equivalent configuration of using three electrodes to measure the mouse ECG has been implemented. Here, the formed injected electrode (i.e. label 1) and another implanted electrode (i.e. label 2) are, respectively utilized as the positive and negative port; while the third electrode (i.e. label 3) is fixed in the left lower limb, serving as an active ground electrode. The label 1 and label 2 electrodes are connected to the MPA acquisition and analysis system, while label 3 electrode is connected to the GND as the counter electrode. The measuring results were displayed and analyzed by the associated software. Furthermore, we adopted a low-pass filter with the cutoff frequency of 150 Hz to improve the SNR (Signal to Noise Ratio) of the recorded signal.

In vivo experimental methods for electrical stimulation using the injectable electrode inside the mouse body. Figure 6c presents the experimental setup for implementing an electrical stimulation to the test mouse. The digital signal generator provides a series of square wave signals with varying magnitudes (the default constants of signal frequency and duty ratio are 10 Hz and 20%, respectively). Meanwhile, the transient ECG signals have been recorded to monitor the subject's responses. Here, the injected electrode (i.e. label 4) is employed as the stimulator electrode to introduce the electrical stimulation into the mouse body. A lead-II mode for measuring the mouse ECG has been implemented. And two implanted electrodes (i.e. label 1 and 2) are, respectively utilized as the positive and negative port; while the third electrode (i.e. label 3) is in the left lower limb, serving as an active ground electrode.

In vivo experimental methods for the electrical stimulation to the sciatic nerves using the injectable electrode. Figure 7a provides a schematic of the experimental setup for loading the electrical stimulations to the sciatic nerve of a frog; here symbols 1, 2 denote the fabricated electrode and sciatic nerve, respectively. In experiment, an interceptive lower part of a bullfrog body was firstly prepared. And we then carry on the fabrication procedure of the injected medical electrode within the frog's tissue, as described in the above paragraph. The two injected electrodes are respectively fabricated in the left and right side of the sciatic nerve near the femur (Fig. 7b). The digital signal generator (Agilent 33250A, Agilent Technologies, U.S.A.) has been used to produce the electric-stimuli signal (Wave form: square-wave, Voltage amplitude: 2 V/4 V, Duty cycle: 20%). During the control experiment, the positive and negative leads of the electric-stimuli signal are directly connected to the targeted tissue. In the experiment I, the positive and negative leads are respectively connected to the injected gelatin; while these two leads are connected to the injectable electrodes, respectively. When loading the electrical stimulation to the nerves, we synchronously applied the video camera (Canon XF305, Canon, Japan) with high spatial and temporal resolution to capture the transient of the frog's gastrocnemius.

1. Irnich, W. Electronic security systems and active implantable medical devices. *Pacing Clin. Electrophysiol.* **25**, 1235–1258 (2002).
2. Adunka, O., Kiefer, J., Unkelbach, M. H., Lehnert, T. & Gstoettner, W. Development and evaluation of an improved cochlear implant electrode. *Laryngoscope* **114**, 1237–1241 (2004).
3. Halperin, D., Kohno, T., Heydt-Benjamin, T. S., Fu, K. & Maisel, W. H. Security and privacy for implantable medical devices. *Pervasive Computing* **7**, 30–39 (2008).
4. Grill, W. M., Norman, S. E. & Bellamkonda, R. V. Implanted neural interfaces: Biochallenges and engineered solutions. *Annu. Rev. Biomed. Eng.* **11**, 1–24 (2009).
5. Fountas, K. N., Kapsalaki, E. & Hadjigeorgiou, G. Cerebellar stimulation in the management of medically intractable epilepsy: A systematic and critical review. *Neurosurg. Focus* **29**, E8 (2010).
6. Zrenner, E. Will retinal implants restore vision? *Science* **295**, 1022–1025 (2002).
7. Maisel, W. H. Consumer protection for patients with implanted medical devices. *N. Engl. J. Med.* **358**, 985–987 (2008).
8. Hlatky, M. A. & Mark, D. B. The high cost of implantable defibrillators. *Eur. Heart J.* **28**, 388–391 (2007).
9. Furno, F. *et al.* Silver nanoparticles and polymeric medical devices: A new approach to prevention of infection? *J. Antimicrob. Chemother.* **54**, 1019–1024 (2004).
10. Langer, R. & Tirrell, D. A. Designing materials for biology and medicine. *Nature* **428**, 487–492 (2004).
11. Frost, M. C., Reynolds, M. M. & Meyerhoff, M. E. Polymers incorporating nitric oxide releasing/generating substances for improved biocompatibility of blood-contacting medical devices. *Biomaterials* **26**, 1685–1693 (2005).
12. Onuki, Y., Bhardwaj, U., Papadimitrakopoulos, F. & Burgess, D. J. A review of the biocompatibility of implantable devices: Current challenges to overcome foreign body response. *J. Diabetes Sci. Technol.* **2**, 1003–1015 (2008).
13. McConnell, G. C. *et al.* Implanted neural electrodes cause chronic, local inflammation that is correlated with local neurodegeneration. *J. Neural. Eng.* **6**, 056003 (2009).
14. Boviatsis, E. J., Stavrinos, L. C., Themistocleous, M., Kouyialis, A. T. & Sakas, D. E. Surgical and hardware complications of deep brain stimulation, a seven-year experience and review of the literature. *Acta. Neurochir.* **152**, 2053–2062 (2010).
15. Sanders, G. D., Hlatky, M. A. & Owens, D. K. Cost-effectiveness of implantable cardioverter-defibrillators. *N. Engl. J. Med.* **353**, 1471–1480 (2005).
16. Grayson, A. C. R. *et al.* A bioMEMS review: MEMS technology for physiologically integrated devices. *Proc. IEEE* **92**, 6–21 (2004).
17. So, J. H. & Dickey, M. D. Inherently aligned microfluidic electrodes composed of liquid metal. *Lab Chip* **11**, 905–911 (2011).
18. So, J. H. *et al.* Reversibly deformable and mechanically tunable fluidic antennas. *Adv. Funct. Mater.* **19**, 1–6 (2009).
19. Zhang, Q., Zheng, Y. & Liu, J. Direct writing of electronics based on alloy and metal ink (DREAM Ink): a newly emerging area and its impact on energy, environment and health sciences. *Front. Energy* **6**, 311–340 (2012).
20. Gao, Y. X., Li, H. Y. & Liu, J. Direct writing of flexible electronics through room temperature liquid metal ink. *PLoS ONE* **7**, e45485 (2012).
21. Li, H. Y., Yang, Y. & Liu, J. Printable tiny thermocouple by liquid metal gallium and its matching metal. *Applied Phys. Lett.* **101**, 073511–1–4 (2012).
22. Siegel, A. C., Bruzewicz, D. A., Weibel, D. B. & Whitesides, G. M. Microsolidics: Fabrication of three-dimensional metallic microstructures in Poly (dimethylsiloxane). *Adv. Mater.* **19**, 727–733 (2007).
23. Kong, T. F., Peng, W. K., Luong, T. D., Nguyen, N. T. & Han, J. Adhesive-based liquid metal radio-frequency microcoil for magnetic resonance relaxometry measurement. *Lab Chip* **12**, 287–294 (2012).
24. Butson, C. R., Moks, C. B. & McIntyre, C. C. Sources and effects of electrode impedance during deep brain stimulation. *Clin. Neurophysiol.* **117**, 447–454 (2006).
25. Chu, V. *et al.* Method for non-invasively recording electrocardiograms in conscious mice. *BMC Physiol.* **1**, 6 (2001).
26. Salama, G. & London, B. Mouse models of long QT syndrome. *J. Physiol.* **578**, 43–53 (2007).
27. Ikada, Y. & Tabata, Y. Protein release from gelatin matrices. *Adv. Drug Deliv. Rev.* **31**, 287–301 (1998).
28. Azab, A. K. *et al.* Biocompatibility evaluation of crosslinked chitosan hydrogels after subcutaneous and intraperitoneal implantation in the rat. *J. Biomed. Mater. Res. A* **83**, 414–422 (2007).
29. Muzzarelli, R. A. A. Genipin-crosslinked chitosan hydrogels as biomedical and pharmaceutical aids. *Carbohydr. Polym.* **77**, 1–9 (2009).
30. Tan, H., Li, H., Rubin, J. P. & Marra, K. G. Controlled gelation and degradation rates of injectable hyaluronic acid-based hydrogels through a double crosslinking strategy. *J. Tissue. Eng. Regen. Med.* **5**, 790–797 (2011).
31. Hallfors, N., Khan, A., Dickey, M. D. & Taylor, A. M. Integration of pre-aligned liquid metal electrodes for neural stimulation within a user-friendly microfluidic platform. *Lab Chip* **13**, 522–526 (2013).
32. Dunne, S. M. & Abraham, R. Dental post-operative sensitivity associated with a gallium-based restorative material. *Brit. Dental J.* **189**, 310–313 (2000).
33. Chen, W. C. *et al.* Role of Gallium-67 scintigraphy in the evaluation of occult sepsis in the medical ICU. *Intern. Emerg. Med.* **7**, 53–58 (2012).
34. Hagemester, F. B., Fesus, S. M., Lamki, L. M. & Haynie, T. P. Role of the gallium scan in Hodgkin's disease. *Cancer* **65**, 1090–1096 (1990).



35. Wataha, J. C. Biocompatibility of dental casting alloys: A review. *J. Prosthet. Dent.* **83**, 223–234 (2000).

Acknowledgments

We appreciate very much the help from Miss Shanshan Zhang and Dr. Yang Yang from Technical Institute of Physics and Chemistry, Chinese Academy of Sciences for preparing the GaInSn-based liquid metal ink and providing the valuable comments to this work.

Author contributions

C.J. designed and performed the experiments, and wrote the manuscript. J.Z. performed the sciatic nerve/gastrocnemius model experiments. X.K.L. provided constructive suggestions

for the packaging material. X.Y.Y. and J.J.L. performed part of the experiments. J.L. conceived the present work, designed the experiments and wrote the manuscript.

Additional information

Supplementary information accompanies this paper at <http://www.nature.com/scientificreports>

Competing financial interests: The authors declare no competing financial interests.

How to cite this article: Jin, C. *et al.* Injectable 3-D Fabrication of Medical Electronics at the Target Biological Tissues. *Sci. Rep.* **3**, 3442; DOI:10.1038/srep03442 (2013).



This work is licensed under a Creative Commons Attribution-NonCommercial-ShareAlike 3.0 Unported license. To view a copy of this license, visit <http://creativecommons.org/licenses/by-nc-sa/3.0>